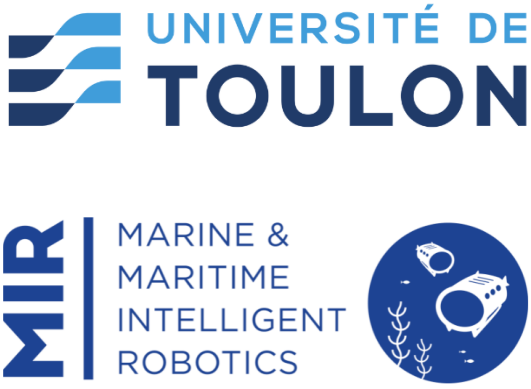

Modeling and control of underwater vehicle: Sparus

By

Mohamed Magdy Atta

Underwater Robotics, Modelling and Control

Submitted to: Prof. Mathieu RICHIER

Universite de Toulon

Contents

1 Introduction

Sparus autonomous underwater vehicle developed by IQUA Robotics in Girona, Spain, is used in a wide range of underwater operations. The following sections will discuss the dynamic modeling of the Sparus vehicle by taking into considerations the stiffness, added mass, and damping effects. In addition, the dynamic model behavior in different underwater scenarios will be analyzed with the help of MATLAB & SIMULINK Simulations.

The Sparus AUV is represented by the figure 1. we consider the origin of the base "body" in the gravity center of the Sparus. It is placed at the x-position of the central thruster and at middle of the cylinder.

$$\vec{r}_g = \begin{bmatrix} 0 \\ 0 \\ 0 \end{bmatrix}_b$$

Moreover, the coordinates of the buoyancy center are:

$$\vec{r}_b = \begin{bmatrix} 0 \\ 0 \\ -0.02\,\mathrm{m} \end{bmatrix}_b$$

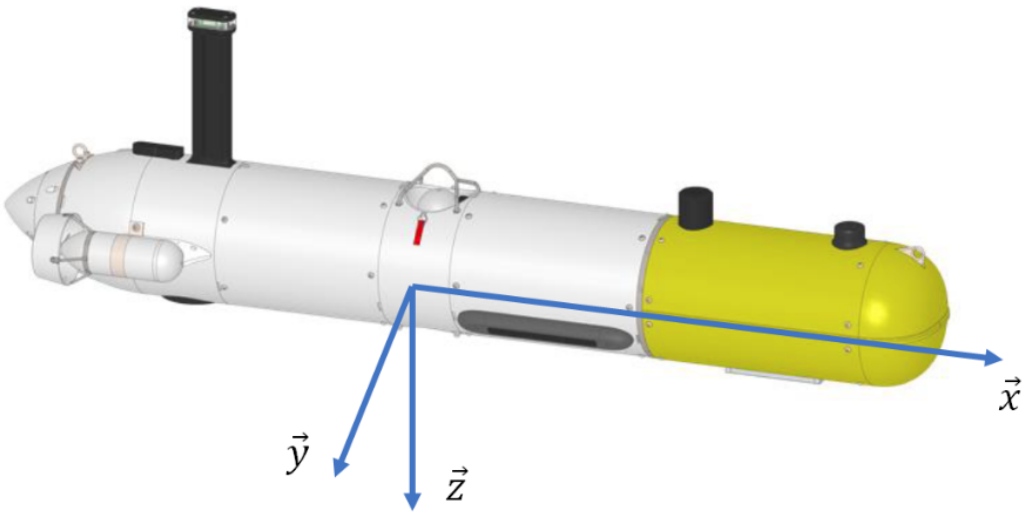

Figure 1: Sparus in 3D

2 Underwater Vehicle Dimensions

The main AUV parts taken into account are the main body, the antenna, and the two thrusters mounted on the two sides of the vehicle. The Sparus dimensions notations and values are shown in fig 2 and table 1.

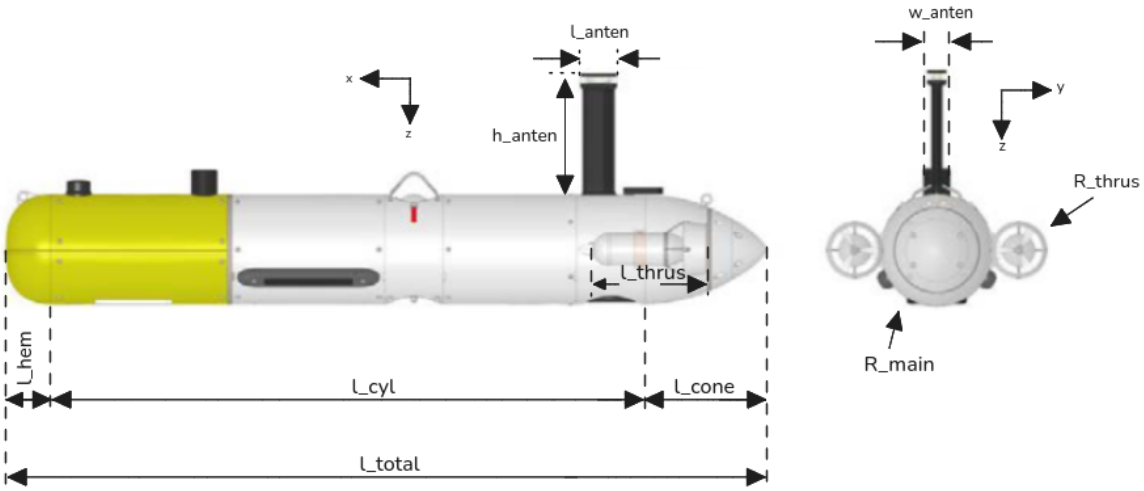

Figure 2: Main Dimensions for Sparus Vehicle

Component	Parameter	Value (m)
Total Length	l_{total}	1.60
Cylinder Length	l_{cyl}	1.25
Hemisphere Length	l_{hem}	0.10
Cone Length	l_{cone}	0.25
Thruster Length	l_{thrus}	0.24
Antenna Length	l_{anten}	0.08
Antenna Width	w_{anten}	0.05
Antenna Height	h_{anten}	0.25
Main Body Radius	R_{main}	0.115
Thruster Radius	R_{thrus}	0.06

Table 1: Dimensions of Sparus AUV Components

3 Global Real Mass Matrix

The global real mass matrix M_{RB}^{CO} is derived based on the Newton–Euler equations of motion for rigid bodies. The matrix is composed of four 3x3 matrices as following:

$$M_{RB}^{CO} = \begin{bmatrix} m\mathbf{I}_{3\times3} & -m\mathbf{S}(\mathbf{r}_g^b) \\ m\mathbf{S}(\mathbf{r}_g^b) & \mathbf{I}_g - m\mathbf{S}^2(\mathbf{r}_g^b) \end{bmatrix} = \begin{bmatrix} 52 & 0 & 0 & 0 & -0.1 & 0 \\ 0 & 52 & 0 & 0.1 & 0 & -1.3 \\ 0 & 0 & 52 & 0 & 1.3 & 0 \\ 0 & 0.1 & 0 & 0.5 & 0 & 0 \\ -0.1 & 0 & 1.3 & 0 & 9.4 & 0 \\ 0 & -1.3 & 0 & 0 & 0 & 9.5 \end{bmatrix}.$$

where:

- $\mathbf{I}_{3\times3}$: 3×3 identity matrix
- m: Mass of the vehicle.
- $\mathbf{I}_g$: Inertia tensor at the center of gravity (CG).
- $\mathbf{S}(\mathbf{r}_g^b)$: Skew-symmetric matrix of the position vector $\mathbf{r}_g^b$.

The first part is the mass matrix $m\mathbf{I}_{3\times3}$:

$$m\mathbf{I}_{3\times3} = \begin{bmatrix} 52 & 0 & 0 \\ 0 & 52 & 0 \\ 0 & 0 & 52 \end{bmatrix}$$

The constant rigid-body mass which is 52 kg across the three degrees of freedom is shown in this matrix .The Sparus vehicle is symmetric, thus the off-diagonal elements of the matrix are set to zeros.

The second part is the inertia matrix $\mathbf{I}_g - m\mathbf{S}^2(\mathbf{r}_g^b)$:

$$\mathbf{I}_g - m\mathbf{S}^2(\mathbf{r}_g^b) = \begin{bmatrix} 0.5 & 0 & 0 \\ 0 & 9.4 & 0 \\ 0 & 0 & 9.5 \end{bmatrix}$$

This matrix shows how the Sparus vehicle resists the rotations around the different axes. It relate the angular moments of the Sparus vehicle to the angular velocities. The inertia around the x-axis is much lower than the inertia around y-axis and z-axis due to the vehicle shape that makes the radius r_x become smaller compared to the radius r_y and r_z during rotation.

The third and forth parts of the global real mass matrix originate from the rotational matrix $m\mathbf{S}(\mathbf{r}_g^b)$:

$$m\mathbf{S}(\mathbf{r}_g^b) = \begin{bmatrix} 0 & 0.1 & 0 \\ -0.1 & 0 & 1.3 \\ 0 & -1.3 & 0 \end{bmatrix}$$

This matrix shows the roll, pitch, and yaw motions that can be generated by the linear accelerations of the Sparus vehicle along the main three axes x, y, and z.

For the roll motion, it is zero when the vehicle accelerates in the x-axis due to moving in straight line. The roll is zero also when accelerating in z-axis since the antenna position do no affect during z-direction movement. When moving in y-direction, there will be a negative roll (-0.1) due to the antenna configuration which will create a clockwise rotation around x-axis.

For the pitch motion, we will have a positive pitch (0.1) when moving in x-direction due to the antenna. There will be no pitch when moving in y-direction. There will be a negative pitch (-1.3) due to the two backward thrusters when moving in z-direction.

For the yaw motion, it is zero when moving in x-direction due to symmetry of the backward thrusters. It is zero when moving in z-direction as well.There will be a positive yaw (1.3) due to the backwark thrusters when moving in y-direction.

4 Added Mass Matrix at global buoyancy center

In fluid dynamics, when a body moves through a fluid and displaces it, the system's global mass is affected and its value increases due to the added mass effect.

The Sparus AUV consists of a number of bodies with different geometries that are forming its ovarall shape and affecting the added mass values during movements underwater. Also, the density of the surrounding fluid affects the added mass values.

The added mass matrix has the same properties of the real mass matrix. The matrix coefficients are:

$$M_A = \begin{bmatrix} X_{\dot{u}} & X_{\dot{v}} & X_{\dot{w}} & X_{\dot{p}} & X_{\dot{q}} & X_{\dot{r}} \\ Y_{\dot{u}} & Y_{\dot{v}} & Y_{\dot{w}} & Y_{\dot{p}} & Y_{\dot{q}} & Y_{\dot{r}} \\ Z_{\dot{u}} & Z_{\dot{v}} & Z_{\dot{w}} & Z_{\dot{p}} & Z_{\dot{q}} & Z_{\dot{r}} \\ K_{\dot{u}} & K_{\dot{v}} & K_{\dot{w}} & K_{\dot{p}} & K_{\dot{q}} & K_{\dot{r}} \\ M_{\dot{u}} & M_{\dot{v}} & M_{\dot{w}} & M_{\dot{p}} & M_{\dot{q}} & M_{\dot{r}} \\ N_{\dot{u}} & N_{\dot{v}} & N_{\dot{w}} & N_{\dot{p}} & N_{\dot{q}} & N_{\dot{r}} \end{bmatrix}^{CB} = \begin{bmatrix} m_{a11} & m_{a12} & m_{a13} & m_{a14} & m_{a15} & m_{a16} \\ m_{a21} & m_{a22} & m_{a23} & m_{a24} & m_{a25} & m_{a26} \\ m_{a31} & m_{a32} & m_{a33} & m_{a34} & m_{a35} & m_{a36} \\ m_{a41} & m_{a42} & m_{a43} & m_{a44} & m_{a45} & m_{a46} \\ m_{a51} & m_{a52} & m_{a53} & m_{a54} & m_{a55} & m_{a56} \\ m_{a61} & m_{a62} & m_{a63} & m_{a64} & m_{a65} & m_{a66} \end{bmatrix}^{CB}$$

The coefficients represent the forces/moments in six degrees of freedom due to linear/angular accelerations in each degree of freedom. For example, a moment in the Y-direction (5) due to an acceleration in the Z-direction (3), $\dot{w}$, is represented by the term $M_{\dot{w}} = m_{53}$.

Assuming the Sparus AUV as a slender body, the added mass can be calculated using the slender body theorem. In addition, the Prolate Spheroid theory is used to determine some coefficients that can not be calculated using the slender body theory.

The main AUV parts taken into account to calculate the added mass matrix are the main body, the antenna, and the two thrusters mounted on the two sides of the vehicle.

Slender body theory works by taking the integration of each part taking into consideration its boundary and shape.

$$m_{aij} = \sum \left[a_{ij}(x) \text{ contributions} \right]$$

For the main body and the two thrusters ,the added mass matrix coefficients are reduced due to the two-plane symmetry as the following:

	1	2	3	4	5	6
1						
2		$m_{22} = \int_L a_{22}\,dx$				$m_{26} = \int_L x\,a_{22}\,dx$
3			$m_{33} = \int_L a_{33}\,dx$		$m_{35} = -\int_L x\,a_{33}\,dx$	
4				$m_{44} = \int_L a_{44}\,dx$		
5			$m_{35} = -\int_L x\,a_{33}\,dx$		$m_{55} = \int_L x^2\,a_{33}\,dx$	
6		$m_{26} = \int_L x\,a_{22}\,dx$				$m_{66} = \int_L x^2\,a_{22}\,dx$

Table 2: Added Mass Matrix for two plane symmetry

For the antenna, the added mass matrix coefficients are reduced due to the three-plane

symmetry as the following:

	1	2	3	4	5	6
1	$m_{11} = \int_L a_{11}\,dx$					
2		$m_{22} = \int_L a_{22}\,dx$				
3						
4				$m_{44} = \int_L a_{44}\,dx$		
5					$m_{55} = \int_L x^2 a_{33}\,dx$	
6						$m_{66} = \int_L x^2 a_{22}\,dx$

Table 3: Added Mass Matrix for Three Plane Symmetry

The calculations for the longitudinal added mass m11 for the main body and thrusters, and m33 for the antenna are done using the Prolate Spheroid theory (Lamb's K-factor).

The added mass matrix is calculated for each component of the Sparus AUV with respect to its center of buoyancy first. Then, except for the main body, each added mass matrix is translated to the global center of buoyancy of the AUV. Finally, the translated matrices are summed up to get the global total added mass matrix at center of buoyancy. The transformations of the mass matrices are expressed as:

$$M^A_{A/a,i} = H^T(\overrightarrow{AB}) M^B_{A/a,i} H(\overrightarrow{AB}),$$

where:

$$H(\overrightarrow{AB}) = \begin{bmatrix} I_3 & S^T \\ 0_3 & I_3 \end{bmatrix},$$

$\overrightarrow{AB}$ defines the relative position of B with respect to A.

S is the skew-symmetric matrix for the vector $\overrightarrow{AB} = [x, y, z]^T$, given by:

$$S = \begin{bmatrix} 0 & -z & y \\ z & 0 & -x \\ -y & x & 0 \end{bmatrix}.$$

Thus, the transformed mass matrix $M^A_{A/a,i}$ is computed as:

$$M^A_{A/a,i} = \begin{bmatrix} I_3 & S^T \\ 0_3 & I_3 \end{bmatrix}^T M^B_{A/a,i} \begin{bmatrix} I_3 & S^T \\ 0_3 & I_3 \end{bmatrix}.$$

4.1 Main body Added Mass Matrix

First, the main body added mass matrix is calculated about the global center of buoyancy. the main body (hull) is composed of three parts; a cone, a cylinder, and a hemisphere. each element in the main body added mass matrix is calculated as the sum of the contributions from the cone, the cylinder, and the hemisphere.

The added mass m_{11} is calculated using the Lamb's K factor according to the following

equations:

$$a = \frac{l_{\text{total}}}{2}, \quad b = R_{\text{main}}, \quad e = \sqrt{1 - \frac{b^2}{a^2}}, \quad \alpha_0 = \frac{2(1-e^2)}{e^3}\left(\frac{1}{2}\ln\left(\frac{1+e}{1-e}\right) - e\right), \quad k_1 = \frac{\alpha_0}{2-\alpha_0}.$$

$$m_{11} = k_1 \cdot \frac{4}{3}\pi\rho ab^2.$$

The other added masses are calculated using the slender body theory. The added masses m_{22} and m_{33} are equal due to symmetry and are calculated as the following:

$$m_{22} = m_{33} = m_{\text{cone}} + m_{\text{cyl}} + m_{\text{hem}}.$$

For the cone contribution:

$$R_{\text{cone}}(x) = \frac{R_{\text{main}}}{l_{\text{cone}}} \cdot \left(x + \frac{l_{\text{total}}}{2} - l_{\text{cone}}\right) + R_{\text{main}}, \quad A_{\text{cone}}(x) = \pi\rho R_{\text{cone}}(x)^2$$

$$m_{22,\text{cone}} = \int_{-\frac{l_{\text{total}}}{2}}^{-\left(\frac{l_{\text{total}}}{2} - l_{\text{cone}}\right)} A_{\text{cone}}(x)\, dx.$$

For the cylinder contribution:

$$A_{\text{cyl}} = \pi\rho R_{\text{main}}^2, \quad m_{22,\text{cyl}} = \int_{-\left(\frac{l_{\text{total}}}{2} - l_{\text{cone}}\right)}^{\frac{l_{\text{total}}}{2} - l_{\text{hem}}} A_{\text{cyl}}\, dx.$$

For the hemisphere contribution:

$$A_{\text{hem}}(x) = \pi\rho\left(l_{\text{hem}}^2 - \left(x - \frac{l_{\text{total}}}{2} + l_{\text{hem}}\right)^2\right), \quad m_{22,\text{hem}} = \int_{\frac{l_{\text{total}}}{2} - l_{\text{hem}}}^{\frac{l_{\text{total}}}{2}} A_{\text{hem}}(x)\, dx.$$

The added masses m_{55} and m_{66} are equal due to symmetry and are calculated as the following:

$$m_{55} = m_{66} = m_{55,\text{cone}} + m_{55,\text{cyl}} + m_{55,\text{hem}}.$$

For the cone contribution:

$$m_{55,\text{cone}} = \int_{-\frac{l_{\text{total}}}{2}}^{-\left(\frac{l_{\text{total}}}{2} - l_{\text{cone}}\right)} x^2 \cdot A_{\text{cone}}(x)\, dx$$

For the cylinder contribution:

$$m_{55,\text{cyl}} = \int_{-\left(\frac{l_{\text{total}}}{2} - l_{\text{cone}}\right)}^{\frac{l_{\text{total}}}{2} - l_{\text{hem}}} x^2 \cdot A_{\text{cyl}}\, dx$$

For the hemisphere contribution:

$$m_{55,\text{hem}} = \int_{\frac{l_{\text{total}}}{2}-l_{\text{hem}}}^{\frac{l_{\text{total}}}{2}} x^2 \cdot A_{\text{hem}}(x)\, dx$$

The off diagonal added masses m_{35}, m_{26}, m_{53}, m_{62} are calculated as the following:

$$m_{35} = m_{53} = -(m_{35,\text{cone}} + m_{35,\text{cyl}} + m_{35,\text{hem}}), \quad m_{26} = m_{62} = -m_{35}.$$

For the cone contribution:

$$m_{35,\text{cone}} = \int_{-\frac{l_{\text{total}}}{2}}^{-\left(\frac{l_{\text{total}}}{2}-l_{\text{cone}}\right)} x \cdot A_{\text{cone}}(x)\, dx$$

For the cylinder contribution:

$$m_{35,\text{cyl}} = \int_{-\left(\frac{l_{\text{total}}}{2}-l_{\text{cone}}\right)}^{\frac{l_{\text{total}}}{2}-l_{\text{hem}}} x \cdot A_{\text{cyl}}\, dx$$

For the hemisphere contribution:

$$m_{35,\text{hem}} = \int_{\frac{l_{\text{total}}}{2}-l_{\text{hem}}}^{\frac{l_{\text{total}}}{2}} x \cdot A_{\text{hem}}(x)\, dx$$

The rotational added mass m_{44} about the x-axis is set to zero due to the symmetry of the geometry which cause minimal movement compared to rotation about y or z-axes.

$$m_{44} = 0.$$

The complete added mass matrix for the main body at global buoyancy center is:

$$M^{CB,global}_{\text{added,main body}} = \begin{bmatrix} m_{11} & 0 & 0 & 0 & 0 & 0 \\ 0 & m_{22} & 0 & 0 & 0 & m_{26} \\ 0 & 0 & m_{33} & 0 & m_{35} & 0 \\ 0 & 0 & 0 & m_{44} & 0 & 0 \\ 0 & 0 & m_{35} & 0 & m_{55} & 0 \\ 0 & m_{26} & 0 & 0 & 0 & m_{66} \end{bmatrix} = \begin{bmatrix} 1.6038 & 0 & 0 & 0 & 0 & 0 \\ 0 & 57.4911 & 0 & 0 & 0 & 3.3190 \\ 0 & 0 & 57.4911 & 0 & -3.3190 & 0 \\ 0 & 0 & 0 & 0 & 0 & 0 \\ 0 & 0 & -3.3190 & 0 & 9.5018 & 0 \\ 0 & 3.3190 & 0 & 0 & 0 & 9.5018 \end{bmatrix}$$

4.2 Thrusters Added Mass Matrix

Secondly, the added mass matrix for the thrusters is calculated with respect to their own center of buoyancy. Each added mass matrix is then translated to the global center of buoyancy of the AUV. Thrusters are considered small bodies compared to the main AUV, thus the coefficients m_{44} , m_{55} , m_{66} , m_{35} are neglected.

The added mass m_{11} is calculated using the Lamb's K factor according to the following

equations:

$$a = \frac{l_{\text{thrus}}}{2}, \quad b = R_{\text{thrus}}, \quad e = \sqrt{1 - \frac{b^2}{a^2}},$$
$$\alpha_0 = \frac{2(1-e^2)}{e^3}\left(\frac{1}{2}\ln\left(\frac{1+e}{1-e}\right) - e\right),$$
$$k_1 = \frac{\alpha_0}{2-\alpha_0}.$$

$$m_{11} = k_1 \cdot \frac{4}{3}\pi\rho ab^2.$$

The added masses m_{22} is equal to zero due to producing very low value compare to the other two axes. The added mass m_{33} are calculated using the slender body theory.

We use the section body of circular cylinder with two fins.

$$A = \pi b^2.$$

$$a = R_{mainbody}$$

$$b = R_{thrus} + R_{mainbody}$$

$$C_A = 1 - (\frac{a}{b})^2 + (\frac{a}{b})^4$$

$$m_{33} = C_A\rho\int_{-l_{thrus}}^{l_{thrus}} A\,dx = C_A\rho\pi b^2 l_{thrus}$$

$$m_{22} = 0, m_{44} = 0, m_{55} = 0, m_{35} = 0, m_{66} = 0, m_{26} = 0$$

The complete added mass matrix for the thrusters at their buoyancy center is:

$$M_{\text{thruster}} = \begin{bmatrix} m_{11} & 0 & 0 & 0 & 0 & 0 \\ 0 & 0 & 0 & 0 & 0 & 0 \\ 0 & 0 & m_{33} & 0 & 0 & 0 \\ 0 & 0 & 0 & 0 & 0 & 0 \\ 0 & 0 & 0 & 0 & 0 & 0 \\ 0 & 0 & 0 & 0 & 0 & 0 \end{bmatrix} = \begin{bmatrix} 0.38 & 0 & 0 & 0 & 0 & 0 \\ 0 & 0 & 0 & 0 & 0 & 0 \\ 0 & 0 & 17.43 & 0 & 0 & 0 \\ 0 & 0 & 0 & 0 & 0 & 0 \\ 0 & 0 & 0 & 0 & 0 & 0 \\ 0 & 0 & 0 & 0 & 0 & 0 \end{bmatrix}$$

The thrusters added mass matrix is then transformed to the global buoyancy center using the transformation equation:

$$M^{CB,global}_{\text{added, thruster}} = \begin{bmatrix} I_3 & S^T(\overrightarrow{AB}) \\ 0_3 & I_3 \end{bmatrix}^T M_{\text{thruster}} \begin{bmatrix} I_3 & S^T(\overrightarrow{AB}) \\ 0_3 & I_3 \end{bmatrix}$$

For the right thruster:

$$\overrightarrow{AB} = r_{\text{buoyancy}} - r_{\text{right thruster}} = \begin{bmatrix} 0 \\ 0 \\ -0.02 \end{bmatrix} - \begin{bmatrix} -0.59 \\ 0.17 \\ 0 \end{bmatrix}$$

$$M^{CB,global}_{\text{added,right thruster}} = \begin{bmatrix} 0.3800 & 0 & 0 & 0 & -0.0076 & 0.0646 \\ 0 & 0 & 0 & 0 & 0 & 0 \\ 0 & 0 & 17.4300 & -2.9631 & -10.2837 & 0 \\ 0 & 0 & -2.9631 & 0.5037 & 1.7482 & 0 \\ -0.0076 & 0 & -10.2837 & 1.7482 & 6.0675 & -0.0013 \\ 0.0646 & 0 & 0 & 0 & -0.0013 & 0.0110 \end{bmatrix}$$

For the left thruster:

$$\overrightarrow{AB} = r_{\text{buoyancy}} - r_{\text{left thruster}} = \begin{bmatrix} 0 \\ 0 \\ -0.02 \end{bmatrix} - \begin{bmatrix} -0.59 \\ -0.17 \\ 0 \end{bmatrix}$$

$$M^{CB,global}_{\text{added,left thruster}} = \begin{bmatrix} 0.3800 & 0 & 0 & 0 & -0.0076 & -0.0646 \\ 0 & 0 & 0 & 0 & 0 & 0 \\ 0 & 0 & 17.4300 & 2.9631 & -10.2837 & 0 \\ 0 & 0 & 2.9631 & 0.5037 & -1.7482 & 0 \\ -0.0076 & 0 & -10.2837 & -1.7482 & 6.0675 & 0.0013 \\ -0.0646 & 0 & 0 & 0 & 0.0013 & 0.0110 \end{bmatrix}$$

4.3 Antenna Added Mass Matrix

Thirdly, the added mass matrix for the antenna is calculated with respect to their own center of buoyancy. The added mass matrix is then translated to the global center of buoyancy of the AUV. Antenna is considered a small body compared to the main AUV, thus the coefficients m_{44} , m_{55} , m_{66} , m_{35} are neglected.

The added mass m_{11} and m_{22} are calculated using the slender body theory.

The added masses m_{33} is equal to zero due to producing very low value compare to the

other two axes.

The added masses m_{11} is calculated as the following:

Area is YZ plane is proportional to w_{anten}

$$m_{11} = \int_{-h_{\text{anten}}/2}^{h_{\text{anten}}/2} A_{\text{rect}}\, dz = \rho w_{\text{anten}} \cdot w_{\text{anten}} \cdot h_{\text{anten}}.$$

The added masses m_{22} is calculated as the following:

Area is XZ plane is proportional to l_{anten}

$$m_{22} = \int_{-h_{\text{anten}}/2}^{h_{\text{anten}}/2} A_{\text{rect}}\, dz = \rho l_{\text{anten}} \cdot l_{\text{anten}} \cdot h_{\text{anten}}.$$

$$m_{33} = 0, m_{44} = 0, m_{55} = 0, m_{35} = 0, m_{66} = 0, m_{26} = 0$$

The complete added mass matrix for the Antenna at its buoyancy center is:

$$M_{\text{antenna}} = \begin{bmatrix} m_{11} & 0 & 0 & 0 & 0 & 0 \\ 0 & m_{22} & 0 & 0 & 0 & 0 \\ 0 & 0 & 0 & 0 & 0 & 0 \\ 0 & 0 & 0 & 0 & 0 & 0 \\ 0 & 0 & 0 & 0 & 0 & 0 \\ 0 & 0 & 0 & 0 & 0 & 0 \end{bmatrix} = \begin{bmatrix} 0.625 & 0 & 0 & 0 & 0 & 0 \\ 0 & 1.60 & 0 & 0 & 0 & 0 \\ 0 & 0 & 0 & 0 & 0 & 0 \\ 0 & 0 & 0 & 0 & 0 & 0 \\ 0 & 0 & 0 & 0 & 0 & 0 \\ 0 & 0 & 0 & 0 & 0 & 0 \end{bmatrix}$$

The antenna added mass matrix is then transformed to the global buoyancy center using the transformation equation:

$$M^{CB,global}_{\text{added, antenna}} = \begin{bmatrix} I_3 & S^T(\overrightarrow{AB}) \\ 0_3 & I_3 \end{bmatrix}^T M_{\text{antenna}} \begin{bmatrix} I_3 & S^T(\overrightarrow{AB}) \\ 0_3 & I_3 \end{bmatrix}$$

$$\overrightarrow{AB} = r_{\text{buoyancy}} - r_{\text{antenna}} = \begin{bmatrix} 0 \\ 0 \\ -0.02 \end{bmatrix} - \begin{bmatrix} -0.39 \\ 0 \\ -(R_{\text{main}} + h_{\text{anten}}/2) \end{bmatrix}$$

$$M^{CB,global}_{\text{added, antenna}} = \begin{bmatrix} 0.6250 & 0 & 0 & 0 & 0.1375 & 0 \\ 0 & 1.6000 & 0 & -0.3520 & 0 & 0.6240 \\ 0 & 0 & 0 & 0 & 0 & 0 \\ 0 & -0.3520 & 0 & 0.0774 & 0 & -0.1373 \\ 0.1375 & 0 & 0 & 0 & 0.0303 & 0 \\ 0 & 0.6240 & 0 & -0.1373 & 0 & 0.2434 \end{bmatrix}$$

The total added mass matrix at the global buoyancy center can be calculated by summing up all the individual components added mass matrices as the following:

$$M^{CB,global}_{\text{added, total}} = M^{CB,global}_{\text{added, main body}} + M^{CB,global}_{\text{added, right thruster}} + M^{CB,global}_{\text{added, left thruster}} + M^{CB,global}_{\text{added, antenna}}$$

$$M^{CB,global}_{\text{added, total}} = \begin{bmatrix} 2.9889 & 0 & 0 & 0 & 0.1223 & 0 \\ 0 & 59.0911 & 0 & -0.3520 & 0 & 3.9430 \\ 0 & 0 & 92.3511 & 0 & -23.8864 & 0 \\ 0 & -0.3520 & 0 & 1.0849 & 0 & -0.1373 \\ 0.1223 & 0 & -23.8864 & 0 & 21.6672 & 0 \\ 0 & 3.9430 & 0 & -0.1373 & 0 & 9.7672 \end{bmatrix}$$

5 Added Mass Matrix at global gravity center

It is assumed that the origin of the base "body" (CO) is in the gravity center (CG) of the Sparus.

The total added mass matrix at global buoyancy center can be transformed to the global gravity center of the Sparus vehicle using the transformation equation defined previously:

$$M^{CG,global}_{\text{added, total}} = \begin{bmatrix} I_3 & S^T(\overrightarrow{AB}) \\ 0_3 & I_3 \end{bmatrix}^T M^{CB,global}_{\text{added, total}} \begin{bmatrix} I_3 & S^T(\overrightarrow{AB}) \\ 0_3 & I_3 \end{bmatrix}$$

$$\overrightarrow{AB} = r_{\text{gravity}} - r_{\text{buoyancy}} = \begin{bmatrix} 0 \\ 0 \\ 0 \end{bmatrix} - \begin{bmatrix} 0 \\ 0 \\ -0.02 \end{bmatrix}$$

$$M^{CG,global}_{\text{added, total}} = \begin{bmatrix} 2.9889 & 0 & 0 & 0 & 0.1821 & 0 \\ 0 & 59.0911 & 0 & -1.5338 & 0 & 3.9430 \\ 0 & 0 & 92.3511 & 0 & -23.8864 & 0 \\ 0 & -1.5338 & 0 & 1.1226 & 0 & -0.2161 \\ 0.1821 & 0 & -23.8864 & 0 & 21.6733 & 0 \\ 0 & 3.9430 & 0 & -0.2161 & 0 & 9.7672 \end{bmatrix}$$

As shown from the matrix values, the rotational matrix values has increased compared to the matrix at the global buoyancy center leading to a higher impact on roll, pitch, and yaw motions generated. Thus it is important to take into consideration the distance between the two points.

6 Values of the Main Solid Compared to the Others

The Sparus vehicle components sizes vary. The main body hull is the largest component and its added mass values is the largest among all the components due to its size. The main body mass matrix values is the highest in all the added mass matrices. The antenna and thrusters rotational matrices values are bigger than the main body ones and has more effect on the generated rotational motions of the vehicle compared to the main body as they resist the motion underwater due to their mounting locations.

7 Added versus Real Mass Matrix

The added mass matrix and the real mass matrix have the same shape and properties, but their components values are different. The values of the added mass matrix are larger than the real mass matrix due to the surrounding water effects on the vehicle during accelerations. The added mass matrix has higher values of the components responsible for rotational motions. In addition, the added mass matrix has two more rotational elements. Thus the added mass matrix affects the roll, pitch, yaw motions more heavier than the real mass matrix coefficients.

8 Drag Matrices

Drag forces are frictional forces that act on an Autonomous Underwater Vehicle (AUV) as it moves through water. These forces arise from the relative motion between the water and the AUV's exterior. Drag forces resist the AUV's motion and play a key role in energy consumption. The global drag force acting on the AUV are given by:

$$D_{\text{drag\_forces}} = D_{NL} \times \left|v^b_{cb/n}\right| \times v^b_{cb/n}$$

where:

- D_{NL} is the drag coefficient matrix.
- $v^b_{cb/n}$ is the speed of the AUV at the.

The drag coefficient matrix D_{NL} at the center of buoyancy is defined as:

$$D_{NL} = \begin{bmatrix} K_{11} & 0 & 0 & 0 & 0 & 0 \\ 0 & K_{22} & 0 & 0 & 0 & 0 \\ 0 & 0 & K_{33} & 0 & 0 & 0 \\ 0 & 0 & 0 & K_{44} & 0 & 0 \\ 0 & 0 & 0 & 0 & K_{55} & 0 \\ 0 & 0 & 0 & 0 & 0 & K_{66} \end{bmatrix}^{CB}$$

The drag coefficients in the matrix D_{NL} are computed as follows:

$$K_{11} = \frac{1}{2}\rho S_x C_{D_{11}}$$

$$K_{22} = \frac{1}{2}\rho C_{D_{22}} D_y L$$

$$K_{33} = \frac{1}{2}\rho C_{D_{33}} D_z L$$

$$K_{44} = 0$$

$$K_{55} = \frac{1}{64}\rho L^4 C_{D_{33}} D_z$$

$$K_{66} = \frac{1}{64}\rho L^4 C_{D_{22}} D_y$$

where:

- ρ is the water density.
- S_x is the projected surface area in the x direction.
- $C_{D_{11}}$ is the 3D drag coefficient in the x direction.

- $C_{D_{22}}$ and $C_{D_{33}}$ are 2D drag coefficients along the y and z directions, respectively.
- D_y and D_z are the characteristic widths in the y and z directions.
- L is the characteristic length of the AUV.

8.1 Drag Matrix for Main body

The drag matrix for the main body of the AUV is derived based on the following parameters and equations:

- $L = 1.6m$: Total hull length
- $R = 0.115$ m: Main body radius
- $\rho = 1000$ kg/m^3: Water density
- $C_{D_{\text{turbulent}}}$: Drag coefficients for turbulent flow
- The projected surface is a circle for motion in x-direction and a rectangle for motions in y and z-directions

$$K_{11} = \frac{1}{2}\pi\rho R^2 C_{D_{\text{turbulent}}}$$

where $C_{D_{\text{turbulent}}} = 0.1$ (Elliptical rod shape)

$$K_{22} = \frac{1}{2}\rho 2RLC_{D_{\text{turbulent}}}$$

where $C_{D_{\text{turbulent}}} = 0.3$ (cylindrical rod shape)

$$K_{33} = K_{22}, \qquad K_{44} = 0$$

$$K_{55} = \frac{1}{64}\rho L^4 C_{D_{\text{turbulent}}}(2R)$$

where $C_{D_{\text{turbulent}}} = 0.3$ (cylindrical rod shape)

$$K_{66} = K_{55}$$

The drag matrix for the main body, $D_{\text{main body}}$, is expressed as:

$$D_{\text{main body}} = \begin{bmatrix} K_{11} & 0 & 0 & 0 & 0 & 0 \\ 0 & K_{22} & 0 & 0 & 0 & 0 \\ 0 & 0 & K_{33} & 0 & 0 & 0 \\ 0 & 0 & 0 & K_{44} & 0 & 0 \\ 0 & 0 & 0 & 0 & K_{55} & 0 \\ 0 & 0 & 0 & 0 & 0 & K_{66} \end{bmatrix} = \begin{bmatrix} 2.0774 & 0 & 0 & 0 & 0 & 0 \\ 0 & 55.20 & 0 & 0 & 0 & 0 \\ 0 & 0 & 55.20 & 0 & 0 & 0 \\ 0 & 0 & 0 & 0 & 0 & 0 \\ 0 & 0 & 0 & 0 & 7.0656 & 0 \\ 0 & 0 & 0 & 0 & 0 & 7.0656 \end{bmatrix}$$

8.2 Drag Matrix for Antenna

The drag matrix for the antenna of the AUV is derived based on the following parameters and equations:

- $h_{\text{anten}} = 0.25m$: Antenna Height
- $l_{\text{anten}} = 0.08m$: Antenna Length
- $w_{\text{anten}} = 0.05m$: Antenna Width
- $\rho = 1000\ \text{kg/m}^3$: Water density
- $C_{D_{\text{turbulent}}}$: Drag coefficients for turbulent flow

$$K_{11} = \frac{1}{2}\rho w_{\text{anten}} h_{\text{anten}} C_{D_{\text{turbulent}}}$$

where $C_{D_{\text{turbulent}}} = 1.9$ (rectangle rod shape)

$$K_{22} = \frac{1}{2}\rho l_{\text{anten}} h_{\text{anten}} C_{D_{\text{turbulent}}}$$

where $C_{D_{\text{turbulent}}} = 1.9$ (rectangle rod shape)

$$K_{33} = 0$$

The antenna size is small compared to the main body, so the coefficients K_{44} , K_{55} , K_{66} are neglected.

$$K_{44} = 0, K_{55} = 0, K_{66} = 0$$

The drag matrix for the antenna, D_{Antenna}, is expressed as:

$$D_{\text{Antenna}} = \begin{bmatrix} K_{11} & 0 & 0 & 0 & 0 & 0 \\ 0 & K_{22} & 0 & 0 & 0 & 0 \\ 0 & 0 & 0 & 0 & 0 & 0 \\ 0 & 0 & 0 & 0 & 0 & 0 \\ 0 & 0 & 0 & 0 & 0 & 0 \\ 0 & 0 & 0 & 0 & 0 & 0 \end{bmatrix} = \begin{bmatrix} 11.875 & 0 & 0 & 0 & 0 & 0 \\ 0 & 19.00 & 0 & 0 & 0 & 0 \\ 0 & 0 & 0 & 0 & 0 & 0 \\ 0 & 0 & 0 & 0 & 0 & 0 \\ 0 & 0 & 0 & 0 & 0 & 0 \\ 0 & 0 & 0 & 0 & 0 & 0 \end{bmatrix}$$

8.3 Drag Matrix for Thrusters

The drag matrix for the thrusters of the AUV is derived based on the following parameters and equations:

- $l_{thrus} = 0.24m$: Thruster length
- $R_{thrus} = 0.06m$: Thruster radius

- $\rho = 1000$ kg/m^3: Water density
- $C_{D_{\text{turbulent}}}$: Drag coefficients for turbulent flow

$$K_{11} = \frac{1}{2}\pi\rho R_{thrus}^2 C_{D_{\text{turbulent}}}$$

where $C_{D_{\text{turbulent}}} = 0.1$ (Elliptical rod shape)

$$K_{33} = \frac{1}{2}\rho 2R_{thrus} l_{thrus} C_{D_{\text{turbulent}}}$$

where $C_{D_{\text{turbulent}}} = 0.3$ (cylindrical rod shape)

$$K_{22} = 0$$

The thrusters size are small compared to the main body, so the coefficients K_{44} , K_{55} , K_{66} are neglected.

$$K_{44} = 0, K_{55} = 0, K_{66} = 0$$

The drag matrix for the thrusters, D_{thruster}, is expressed as:

$$D_{\text{thruster}} = \begin{bmatrix} K_{11} & 0 & 0 & 0 & 0 & 0 \\ 0 & 0 & 0 & 0 & 0 & 0 \\ 0 & 0 & K_{33} & 0 & 0 & 0 \\ 0 & 0 & 0 & 0 & 0 & 0 \\ 0 & 0 & 0 & 0 & 0 & 0 \\ 0 & 0 & 0 & 0 & 0 & 0 \end{bmatrix} = \begin{bmatrix} 0.5655 & 0 & 0 & 0 & 0 & 0 \\ 0 & 0 & 0 & 0 & 0 & 0 \\ 0 & 0 & 4.320 & 0 & 0 & 0 \\ 0 & 0 & 0 & 0 & 0 & 0 \\ 0 & 0 & 0 & 0 & 0 & 0 \\ 0 & 0 & 0 & 0 & 0 & 0 \end{bmatrix}$$

9 Simulations and Experiments

After having our mathematical model for the Sparus, a Matlab and Simulink simulation is performed. The simulation allows us to generate different motions for the Sparus using three thrusters; one aligned with z-axis, and the other two aligned with x-axis. After running the simulation, we analyze the behavior and response of the Sparus to different underwater operational scenarios. We use the output poses, velocities, and accelerations for analysis.To simulate different scenarios, we vary the percentage of each thruster maximum input force applied to the Sparus vehicle. Also, we adjust the initial positions and velocities.

Our z-axis positive direction is pointing downward. To validate the simulator, we start first by testing the buoyancy behavior of the vehicle by setting the thrusters activation to [0 0 0] and the initial positions to [0 0 5 0 pi/2 0]. In this scenario we have our thrusters deactivated and the initial z position is +5 and the initial pitch orientation is 90 degrees. We got the following plots after running the simulation for 120 seconds:

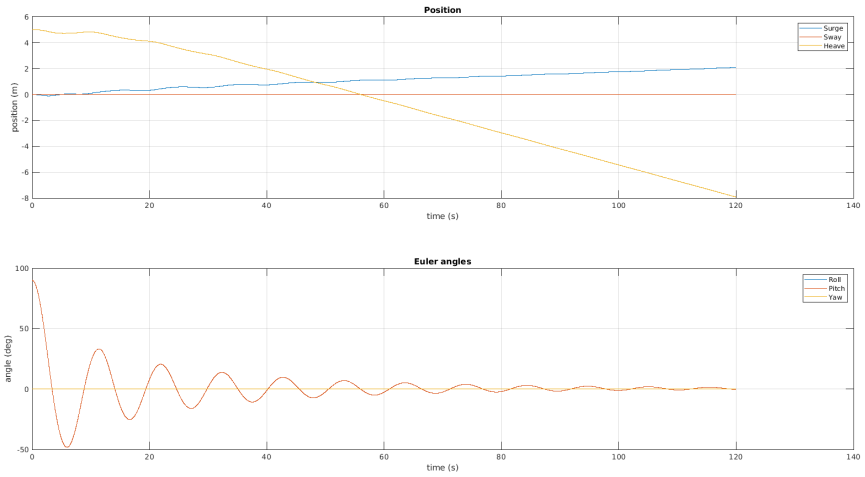

Figure 3: Buoyancy Behavior

As seen in figure [3], the buoyancy effect happened as predicted. The vehicle started to move upward from its initial z-position to be able to float. Also, the Sparus adjusted its orientation from the initial 90 degrees pitch angle to around 0 degree pitch angle due to hydrostatic equilibrium. This is because the center of buoyancy is above the center of gravity, which creates a restoring moment that aligns the Sparus vehicle horizontally.

Secondly, we tested the heave motion along z-axis by setting the thrusters activation to [100 0 0] and the initial positions and velocities to zeros. In this scenario we have only our first thruster aligned with z-axis activated and the other two thrusters deactivated. We got the following plot after running the simulation for 50 seconds:

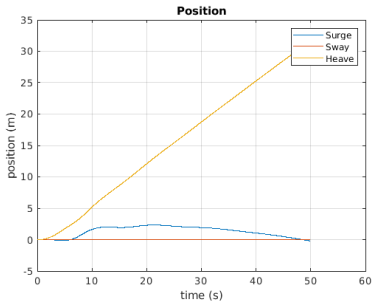

Figure 4: Heave Motion

As seen in figure [4], the movement in z-direction happened as predicted. The Sparus started to move downwards in the positive z-direction and going deeper into the water.

Thirdly, we will analyze the impact of the different coefficients in the global mass matrix. The values of the coefficients in the global mass matrix are shown below:

$$M^{CG}_{\text{global}} = M^{CG}_{\text{added}} + M^{CG}_{\text{real}}$$

$$M^{CG}_{\text{global}} = \begin{bmatrix} m_{11} & m_{12} & m_{13} & m_{14} & m_{15} & m_{16} \\ m_{21} & m_{22} & m_{23} & m_{24} & m_{25} & m_{26} \\ m_{31} & m_{32} & m_{33} & m_{34} & m_{35} & m_{36} \\ m_{41} & m_{42} & m_{43} & m_{44} & m_{45} & m_{46} \\ m_{51} & m_{52} & m_{53} & m_{54} & m_{55} & m_{56} \\ m_{61} & m_{62} & m_{63} & m_{64} & m_{65} & m_{66} \end{bmatrix} = \begin{bmatrix} 54.9889 & 0 & 0 & 0 & 0.0821 & 0 \\ 0 & 111.0911 & 0 & -1.4338 & 0 & 2.6430 \\ 0 & 0 & 144.3511 & 0 & -22.5864 & 0 \\ 0 & -1.4338 & 0 & 1.6226 & 0 & -0.2161 \\ 0.0821 & 0 & -22.5864 & 0 & 31.0733 & 0 \\ 0 & 2.6430 & 0 & -0.2161 & 0 & 19.2672 \end{bmatrix}$$

We first tested the behavior of the Sparus when imposing linear acceleration along the x-direction by setting the thrusters activation to [0 15 15] and the initial positions and velocities to zeros. In this scenario we have only our second and third thrusters aligned with x-axis activated and the z-axis thruster is deactivated. We got the following plots after running the simulation for 20 seconds:

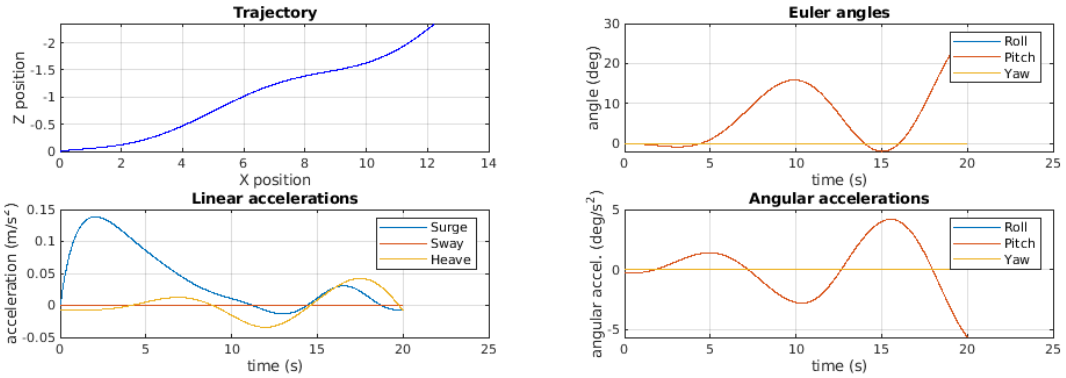

Figure 5: Imposing linear acceleration along x-axis

As seen in figure [5], the trajectory subplot shows that the movement in x-direction

happened as predicted in the coefficient m_{11} in the global mass matrix due to the imposed linear acceleration along x-axis, but there was also movements upward in the z-direction. This behavior happened due to the effect of the antenna position creating a pitch angle during motion as shown in the Euler angles subplot. The simulated behavior happened due to the coefficient m_{51} in the global mass matrix, which indicates that a moment around y-axis is generated when a linear acceleration along x-axis is applied. Also, the angular accelerations subplot shows that an angular acceleration around y-axis was generated, which in turns generates a force in z-direction as shown in the coefficient m_{35}. The linear accelerations subplot shows that there are an acceleration in the x-direction as predicted, but it shows also an oscillating values of the acceleration in z-direction due to the oscillating pitch angle during motion as shown in the Euler angles subplot.

Next, we tested the behavior of the Sparus when imposing linear acceleration along the z-direction by setting the thrusters activation to [10 0 0] and the initial positions and velocities to zeros. In this scenario we have only our first thruster aligned with z-axis activated and the other two thrusters deactivated. We got the following plots after running the simulation for 100 seconds:

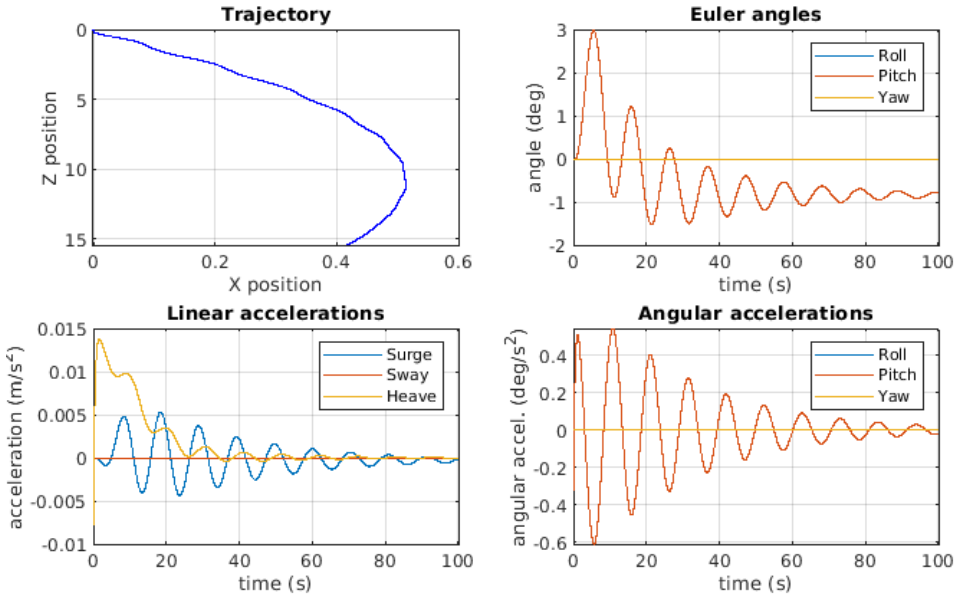

Figure 6: Imposing linear acceleration along z-axis

As seen in figure [6], the trajectory subplot shows that the movement in the z-direction happened as predicted in the coefficient m_{33} in the global mass matrix due to the imposed linear acceleration along z-axis, but there was also movements in the x-direction. This behavior happened due to the effect of the second and third backward thrusters positions creating a pitch angle during motion as shown in the Euler angles subplot. The simulated behavior happened due to the coefficient m_{53} in the global mass matrix, which indicates

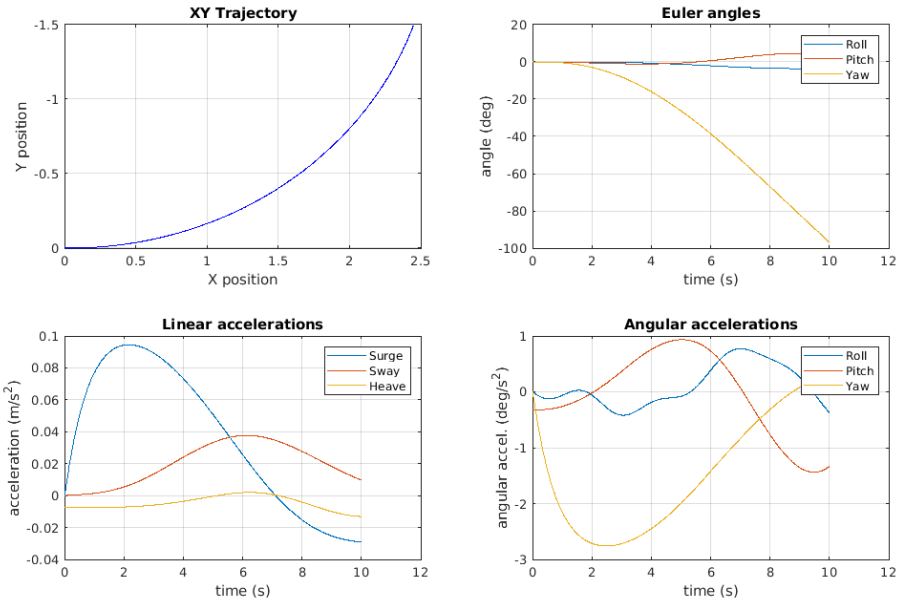

Figure 7: Activation of Right Backward Thruster only

As seen in figure [7], the trajectory subplot shows that the movement in the negative y-direction happened as predicted due to only activating the right backward thruster. Also, the position of the right thruster created a yaw angle during motion as shown in the Euler angles subplot. The angular accelerations subplot shows this angular acceleration around z-axis which created a motion in y-direction as indicated in the coefficient m_{26} in the global mass matrix. The linear accelerations subplot shows that there are an acceleration in the x-direction as predicted,in the coefficient m_{11} in the global mass matrix due to the right thruster being aligned with the x-axis.

Finally, we will analyze the impact of the drag forces of the different bodies. We will observe the damping behavior of the Sparus by impose constant linear speed on different scenarios.

First of all we set all the thrusters activations to zero and set the initial speed value along the x-axis to 10. we tested the damping when all drag forces are added and when all of them except the antenna drag force are added. We got the following plots after running the simulation for 30 seconds:

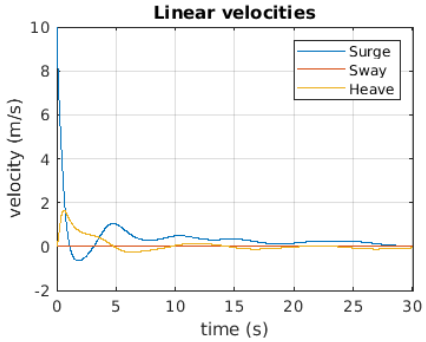

Figure 8: Simulation with all drag forces

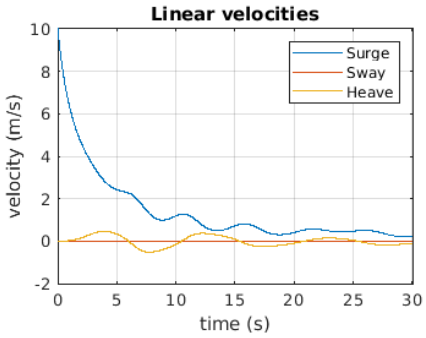

Figure 9: Simulation with all drag forces except antenna

As seen in both figure [8] and figure [9], the velocities plots shows that the speed in the x-direction is decreasing over time indicating that the drag forces is damping the motion. In the simulation in figure [8], the velocity is decaying faster than the simulation in figure [9] due to the antenna drag force being added in figure [8].

Secondly, we set all the thrusters activations to zero and set the initial speed value along the x-axis to 10. we tested the damping when all drag forces are neglected and got the following plots after running the simulation for 30 seconds:

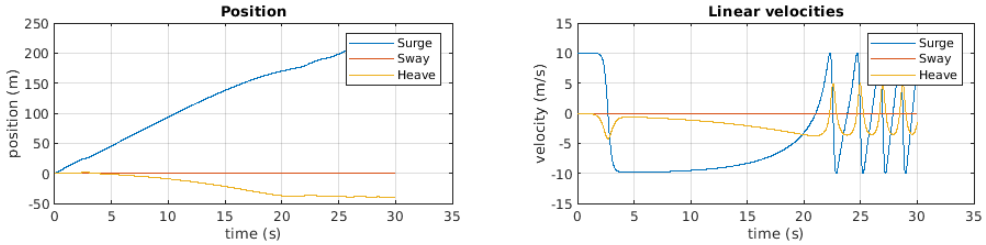

Figure 10: Simulation without the drag forces

As seen in figure [10], the velocities subplot shows that the speed in the x-direction keeps oscillating without damping due to the absence of the drag forces, especially the main body force. In the position subplot, we can see that the Sparus motion in the forward x-direction keeps increasing over time as the velocity values along the x-axis is not decaying.

When testing the heave downwards motion and checking the effect of removing the two backwards thrusters drag forces, we did not notice a big difference in damping z-axis velocity.